JNCI J Natl Cancer Inst (2017) 109(11): djx065

doi: 10.1093/jnci/djx065
First published online June 3, 2017
Article

ARTICLE

An ERBB1-3 Neutralizing Antibody Mixture With High Activity Against Drug-Resistant HER2+ Breast Cancers With ERBB Ligand Overexpression

Luis J. Schwarz, Katherine E. Hutchinson, Brent N. Rexer, Mónica Valeria Estrada, Paula I. Gonzalez Ericsson, Melinda E. Sanders, Teresa C. Dugger, Luigi Formisano, Angel Guerrero-Zotano, Monica Red-Brewer, Christian D. Young, Johan Lantto, Mikkel W. Pedersen, Michael Kragh, Ivan D. Horak, Carlos L. Arteaga

Affiliations of authors: Department of Medicine (LJS, KEH, BNR, TCD, LF, AGZ, MRB, CDY, CLA) and Department of Pathology, Microbiology and Immunology (MES), Vanderbilt University Medical Center, Nashville, TN; Breast Cancer Research Program, Vanderbilt-Ingram Cancer Center, Nashville, TN (MVE, PGE, MES, CLA); Department of Cancer Biology, Vanderbilt University, Nashville, TN (CLA); Symphogen, Ballerup, Denmark (JL, MWP, MK, IDH).

Correspondence to: Carlos L. Arteaga, MD, Division of Oncology, VUMC, 2220 Pierce Avenue, 777 PRB, Nashville, TN 37232-6307 (e-mail: carlos.arteaga@vanderbilt.edu).

Abstract

Background: Plasticity of the ERBB receptor network has been suggested to cause acquired resistance to anti–human epidermal growth factor receptor 2 (HER2) therapies. Thus, we studied whether a novel approach using an ERBB1-3-neutralizing antibody mixture can block these compensatory mechanisms of resistance.

Methods: HER2+ cell lines and xenografts ($n \geq 6$ mice per group) were treated with the ERBB1-3 antibody mixture Pan-HER, trastuzumab/lapatinib (TL), trastuzumab/pertuzumab (TP), or T-DM1. Downregulation of ERBB receptors was assessed by immunoblot analysis and immunohistochemistry. Paired pre- and post-T-DM1 tumor biopsies from patients ($n = 11$) with HER2-amplified breast cancer were evaluated for HER2 and P-HER3 expression by immunohistochemistry and/or fluorescence in situ hybridization. ERBB ligands were measured by quantitative reverse transcription polymerase chain reaction. Drug-resistant cells were generated by chronic treatment with T-DM1. All statistical tests were two-sided.

Results: Treatment with Pan-HER inhibited growth and promoted degradation of ERBB1-3 receptors in a panel of HER2+ breast cancer cells. Compared with TL, TP, and T-DM1, Pan-HER induced a similar antitumor effect against established BT474 and HCC1954 tumors, but was superior to TL against MDA-361 xenografts (TL mean = 2026 mm^3, SD = 924 mm^3, vs Pan-HER mean = 565 mm^3, SD = 499 mm^3, $P = .04$). Pan-HER-treated BT474 xenografts did not recur after treatment discontinuation, whereas tumors treated with TL, TP, and T-DM1 did. Post-TP and post-T-DM1 recurrent tumors expressed higher levels of neuregulin-1 (NRG1), HER3 and P-HER3 (all $P < .05$). Higher levels of P-HER3 protein and NRG1 mRNA were also observed in HER2+ breast cancers progressing after T-DM1 and trastuzumab (NRG1 transcript fold change ± SD; pretreatment = 2, SD = 1.9, vs post-treatment = 11.4, SD = 10.3, $P = .04$). The HER3-neutralizing antibody LJM716 resensitized the drug-resistant cells to T-DM1, suggesting a causal association between the NRG1-HER3 axis and drug resistance. Finally, Pan-HER treatment inhibited growth of HR6 trastuzumab- and T-DM1-resistant xenografts.

Conclusions: These data suggest that upregulation of a NRG1-HER3 axis can mediate escape from anti-HER2 therapies. Further, multitargeted antibody mixtures, such as Pan-HER, can simultaneously remove and/or block targeted ERBB receptor and ligands, thus representing an effective approach against drug-sensitive and -resistant HER2+ cancers.

Received: September 8, 2016; **Revised:** February 3, 2017; **Accepted:** March 15, 2017

Pan-HER is a novel antibody mixture identified by a systematic screen of the optimal combination of antibodies simultaneously targeting two nonoverlapping epitopes within each epidermal growth factor receptor (EGFR), HER2 and HER3. Pan-HER exhibits superior activity against a broad panel of cell lines and patient-derived xenografts (PDXs) from diverse genetic backgrounds compared with cetuximab, trastuzumab, and the HER3 antibody seribantumab (MM-121) (1,2). Treatment with Pan-HER promotes the formation of large clusters of cross-linked receptors on the cell surface, inducing sustained receptor internalization that, over time, reduces recycling and increases degradation of targeted receptors, thus potentially overcoming drug resistance caused by acquired mutations, ERBB ligand overexpression, and/or compensatory ERBB receptor upregulation (3,4).

Increased expression of the ERBB ligands EGF, TGFα, BTC, and NRG1 has been shown to reduce the antitumor effect of the HER2 antibody trastuzumab against HER2-overexpressing (HER2+) breast cancer cells (5). Furthermore, cells with acquired resistance to trastuzumab express higher ERBB ligand levels and EGFR/HER2 and HER2/HER3 heterodimers (6). This resistance is anticipated as trastuzumab, which binds to an epitope in domain IV of the HER2 ectodomain, a region uninvolved with receptor dimerization, is unable to prevent ERBB ligand-induced HER2-containing heterodimers (7). Consistent with this notion, NRG1 has been shown to rescue HER2+ breast cancer cells from the cytotoxic effect of T-DM1, an antibody-drug conjugate where trastuzumab is linked to cytotoxic chemotherapy (8). The addition of pertuzumab, a monoclonal antibody that binds the dimerization domain II of HER2, overcomes NRG1-induced resistance to trastuzumab and T-DM1 (9,10).

Adaptive changes to HER2 blockade with trastuzumab also involve compensatory upregulation and/or activation of ERBB coreceptors. In HR5 and HR6 cells derived from BT474 xenografts with acquired resistance to trastuzumab in vivo, we observed increased levels of phosphorylated/activated EGFR and HER3 (6). Similar changes were found in a panel of breast cancer cell lines chronically maintained under treatment with trastuzumab (11). Further, even dual HER2 blockade with trastuzumab and the EGFR/HER2 tyrosine kinase inhibitor (TKI) lapatinib is unable to completely block compensatory HER3 function. In this case, the addition of a neutralizing HER3 antibody was shown to synergize with the combination of trastuzumab and lapatinib against HER2+ xenografts (12). We hypothesized that the simultaneous blockade of EGFR, HER2, and HER3 with Pan-HER would prevent these escape mechanisms in HER2+ breast cancer cells and tumors.

Methods

Xenograft Studies

Xenograft experiments were conducted using four-week-old female athymic mice (n ≥ 6 mice per group). All mouse experiments were approved by the Vanderbilt Institutional Animal Care and Use Committee, protocol No. M/14/028. Detailed analysis of procedures can be found in the Supplementary Methods (available online).

Tumor Biopsies and Patients

Formalin-fixed, paraffin-embedded (FFPE) tumor blocks were from a cohort of patients (n = 11) who had consented to the use of any de-identified tumor tissues for research purposes under the auspices of an institutional review board–approved protocol (Vanderbilt Institutional Review Board No. 160606). Selection criteria is described in the Supplementary Methods (available online).

Statistical Analysis

Paired and unpaired *t* tests were used to determine statistically significant differences in cell proliferation assays, in vivo tumor growth assays, real-time quantitative reverse transcription polymerase chain reaction (qRT-PCR) assays, and H-scores (immunohistochemistry). A *P* value of less than .05 was considered statistically significant, and all statistical tests were two-sided. Bar graphs show mean ± SD, unless otherwise stated in the figure legend.

Additional methods are available in the Supplementary Methods (available online).

Results

ERBB Receptor Downregulation and Cell Viability

We first evaluated the growth inhibitory activity of Pan-HER using a panel of seven HER2+ breast cancer cell lines growing in Matrigel-embedded 3D culture (hereafter called 3D Matrigel). MDA-361, MDA-453, HCC1954, UACC893, and SUM190PT cells contain activating mutations in the catalytic (H1047R) or helical domain (E545K) of *PIK3CA*. All five cell lines with *PIK3CA* mutations were relatively insensitive to trastuzumab, but growth of four of these cell lines (MDA-361, UACC893, HCC1954, and MDA-453; all $P \leq .05$) was inhibited by Pan-HER (Figure 1A). SUM190PT cells, derived from an inflammatory breast cancer, were refractory to both treatments.

We next compared the efficacy of Pan-HER with that of anti-HER2 drug combinations and T-DM1. Pan-HER was superior to the combination of trastuzumab and pertuzumab (TP) against HER2+/PIK3CA mutant cells vs untreated control: HCC1954 (mean = 83.45%, SD = 10.09%, vs 15.86%, SD = 10.72%, $P < .001$), UACC893 (mean = 42.55%, SD = 6.88%, vs 21.82%, SD = 2.40%, $P = .01$), and MDA-453 (mean = 68.05%, SD = 9.03%, vs 35.08%, SD = 5.33, $P = .03$) (Figure 1B). T-DM1 had the strongest growth-inhibitory effect against all cell lines. Growth inhibition induced by Pan-HER was associated with time-dependent internalization and degradation of EGFR, HER2, and HER3 receptors (Figure 1C); Pan-HER-induced ERBB receptor downregulation was more extensive compared with TP or T-DM1 (Figure 1D). These results suggest that treatment with Pan-HER diminished cell surface levels of EGFR, HER2, and HER3 independent of *PIK3CA* mutation status.

ERBB Receptor Downregulation and Inhibition of Tumor Growth In Vivo

We next established BT474, HCC1954, and MDA-361 xenografts in nude mice and compared the in vivo activity of Pan-HER to other approved anti-HER2 therapies. Mice with established tumors measuring at least 500 mm^3 were randomly assigned to treatment with vehicle, trastuzumab and lapatinib (TL), TP, T-DM1, or Pan-HER. All treatments were effective across the panel of xenografts (Figure 2, A–C). In mice with MDA-361 tumors, Pan-HER and TP were superior to TL (mean tumor volume in mm^3 ± SD; TL mean = 2026 mm^3, SD = 924 mm^3, vs Pan-HER mean = 565 mm^3, SD = 499 mm^3, $P = .04$) (Figure 2C).

ARTICLE

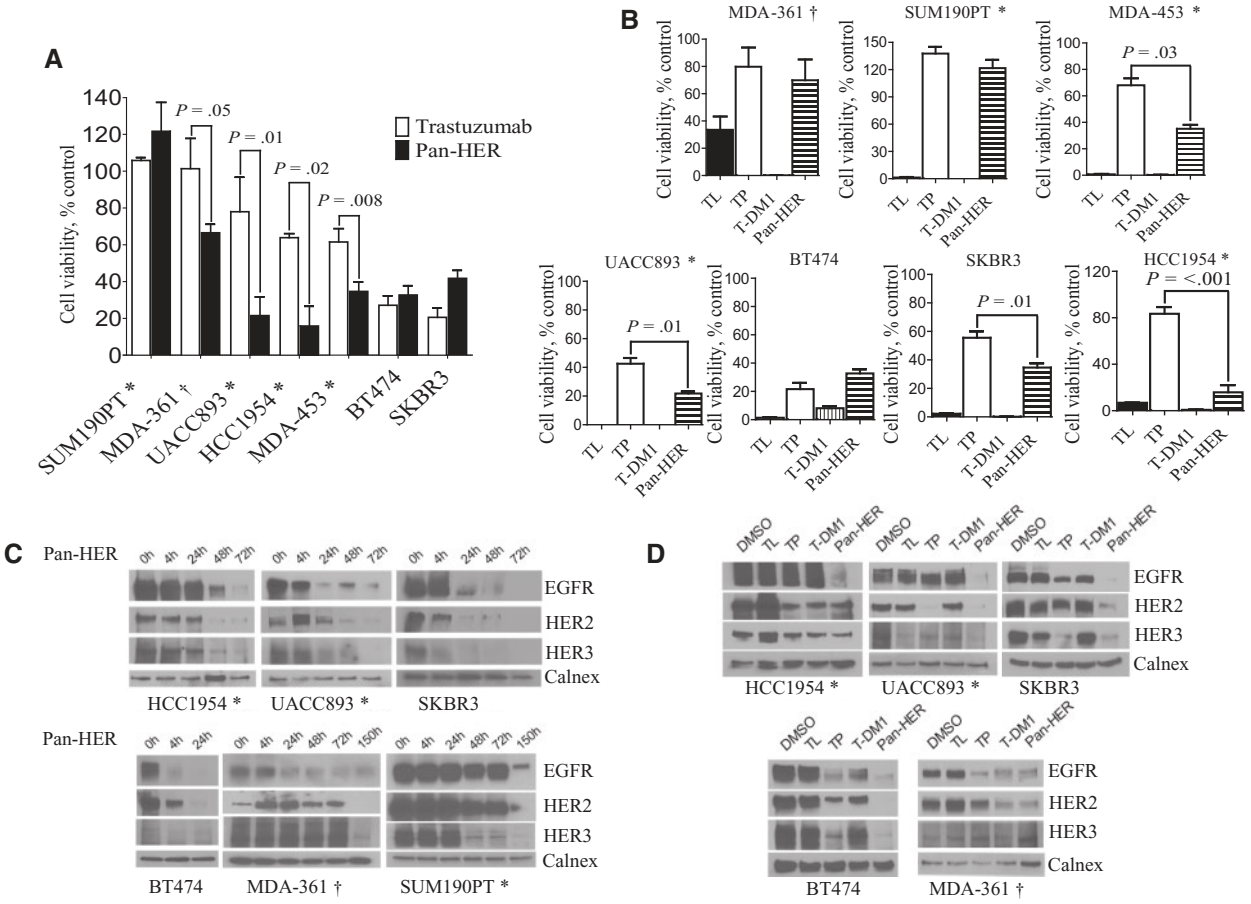

Figure 1. In vitro antitumor activity of Pan-HER against HER2+ breast cancer cells. **A)** Cells (~1x10^4) were seeded in 48-well plates in triplicate in 3D Matrigel plus their respective growth medium and treated with trastuzumab 20 μg/mL or Pan-HER 20 μg/mL for 12 days; fresh medium and inhibitors were replenished every three days. Cell viability was measured by MTT assay and quantified by GelCount. Each **bar** represents mean ± SD relative to untreated controls (n = 3, mean % viability ± SD for trastuzumab/Pan-HER. Two-tailed paired *t* tests were performed to calculate *P* values. **B)** Cells (~1x10^4) were seeded in 48-well plates in triplicate in 3D Matrigel plus their respective growth medium and treated with trastuzumab 20 μg/mL + lapatinib 1 μM (TL), trastuzumab 20 μg/mL + pertuzumab 20 μg/mL (TP), T-DM1 1 μg/mL, or Pan-HER 20 μg/mL; fresh medium and drugs were replenished every three days. On day 12, colonies were stained with MTT and quantified by GelCount. Each **bar** represents the mean cell viability ± SD relative to untreated controls (n = 3, mean % viability ± SD for TP/Pan-HER). Two-tailed paired *t* tests were performed to calculate *P* values. **C)** Cells were treated with Pan-HER 20 μg/mL over the indicated time course and then cell surface biotinylated for 30 minutes at 4°C. Cell lysates were prepared and precipitated with immobilized NeutrAvidin gel; eluates were separated by SDS-PAGE and subjected to immunoblot analysis with the indicated antibodies. **D)** Cells were treated with DMSO or the same concentrations of TL, TP, T-DM1, or Pan-HER as in **(B)** and then biotinylated as described in **(C)**. After 72 hours, cells were harvested; lysates were prepared, separated by SDS-PAGE, and subjected to immunoblot analyses with EGFR, HER2, HER3, and Calnex (control) antibodies. *H1047R mutation and †E545K mutation. EGFR = epidermal growth factor receptor; TL = trastuzumab/lapatinib; TP = trastuzumab/pertuzumab.

Immunoblot analysis confirmed statistically significant down-regulation of EGFR, HER2, and HER3 in MDA-361 and BT474 xenografts (Figures 2D and Supplementary Figure 1A, available online, for MDA-361 and BT474 xenografts, respectively), except for HER2 in HCC1954 xenografts (Supplementary Figure 1B, available online). Altogether, cell surface biotinylation confirmed that Pan-HER enhances internalization of ERBB receptors as a first step in the process of antibody-induced receptor degradation, while immunoblot analysis captures different stages of this process (internalization, endocytosis, and degradation), thus potentially explaining the variability observed on ERBB receptor levels after anti-HER2 treatment of mouse xenografts.

After a complete response of BT474 and HCC1954 xenografts, treatment was discontinued and mice were followed for tumor recurrence. Among mice with BT474 xenografts treated with TP, TL, and T-DM1, 25% to 50% of mice exhibited a tumor recurrence within 50 weeks of follow-up, while no xenograft regrowth was observed among mice that had been treated with Pan-HER (Figure 2A; Supplementary Table 1, available online). In three mice, HCC1954 xenografts recurred after having achieved a complete response to T-DM1, while the other four mice remained tumor free up to 50 days (Figure 2B).

ERBB Receptors and Ligands in Drug-Resistant HER2+ Xenografts and Primary Tumors

We and others have previously shown the critical role of HER3 and ERBB ligands in acquired resistance to anti-HER2 therapies (6,12–14). Thus, we examined ERBB receptor and ligand levels by immunohistochemistry (IHC) and qPCR, respectively. BT474 tumors recurring after TP and T-DM1 retained their histological features by hematoxylin and eosin staining, but exhibited statistically significantly higher HER3 (mean H-score ± SD; untreated = 85, SD = 10; post-TP = 138, SD = 24; post-T-DM1 = 143.3, SD = 2.8; $P = .03$ for untreated vs post-TP and $P = .01$ for untreated vs

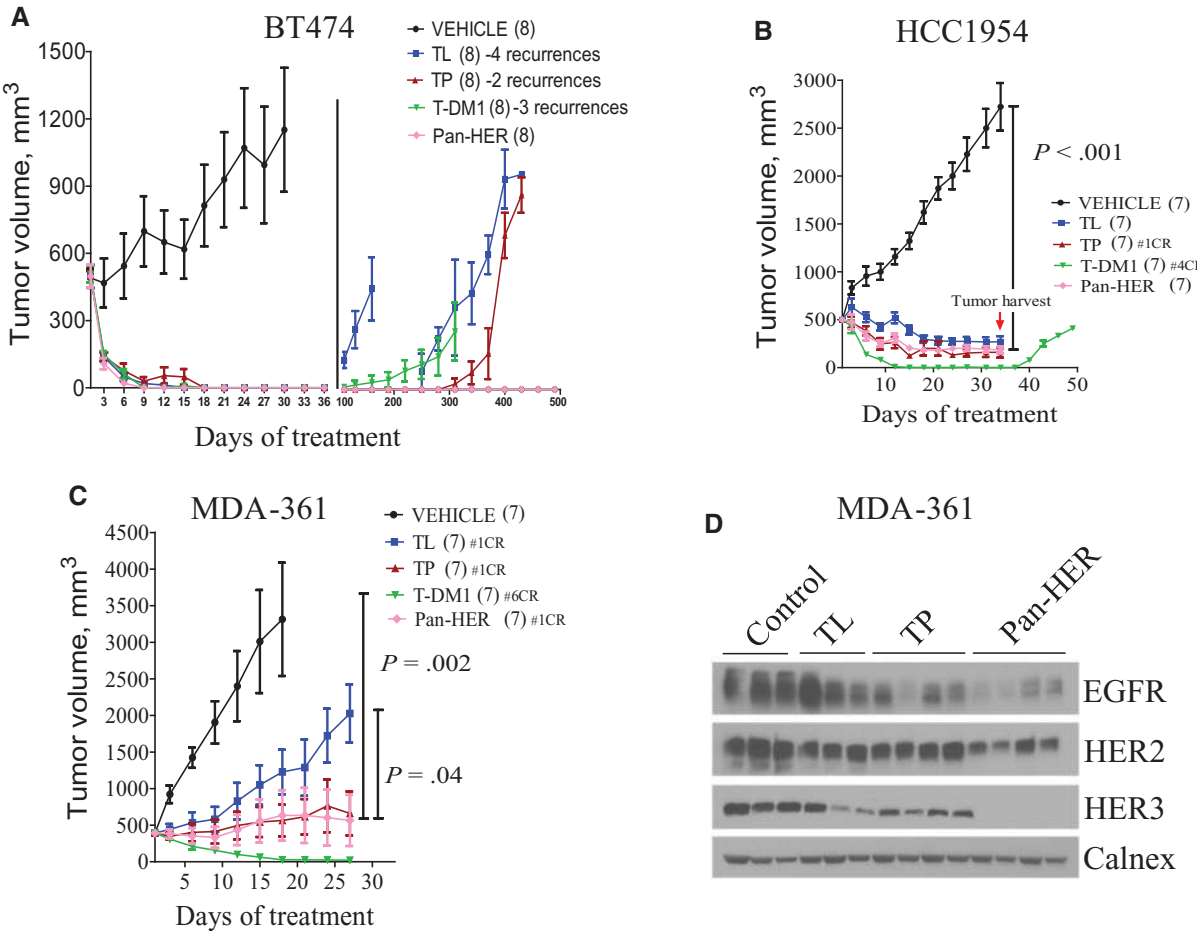

Figure 2. Pan-HER–induced ERBB receptor downregulation and antitumor action in vivo. **A–C)** BT474, HCC1954, and MDA-361 cells were injected subcutaneously in the dorsum of female athymic mice. Mice bearing tumors 500 mm^3 in size or larger were randomly assigned to treatment with 1) vehicle, 2) trastuzumab 30 mg/kg by intraperitoneal (i.p.) injection twice a week and lapatinib 100 mg/kg by orogastric gavage once a day, 3) trastuzumab and pertuzumab 30 mg/kg by i.p. injection twice a week, 4) T-DM1 15 mg/kg intravenously by single tail vein injection, or 5) Pan-HER 50 mg/kg by i.p. injection three times a week. Numbers of mice per treatment arm are shown **in parentheses**. Each data point represents mean tumor volume in mm^3 ± SD. Two-tailed paired *t* tests were performed to calculate *P* values. In mice bearing BT474 tumors, treatment was discontinued on day 21; mice were then followed up to 400 days for recurrence. **D)** MDA-361 xenografts were harvested at the end of the treatment, four hours after the last dose of lapatinib and 24 hours after the last dose of any of the antibodies. CR = number of complete responses; EGFR = epidermal growth factor receptor; TL = trastuzumab/lapatinib; TP = trastuzumab/pertuzumab.

ARTICLE

post-T-DM1) and P-HER3 protein levels (mean H-score ± SD; untreated = 13.3, SD = 10.4; post-TP = 66, SD = 26.9; post-T-DM1 = 91.7, SD = 33.3; $P = .05$ for untreated vs post-TP and $P = .03$ for untreated vs post-T-DM1) (Figure 3, A and B). mRNA levels of NRG1 (fold change ± SD; untreated = 0.43, SD = 0.17; post-TP = 0.99, SD = 0.12; and post-T-DM1 = 1.59, SD = 0.14; $P = .03$ for untreated vs post-TP and $P = .02$ for untreated vs post-T-DM1) and TGFα (fold change ± SD; untreated = 0.88, SD = 0.2; vs post-T-DM1=1.5, SD = 0.1; $P = .02$) also were statistically significantly higher (Figure 3B). Tumors recurring after TL treatment had no statistically significant change in ERBB receptor or ligand expression (data not shown). HCC1954 xenografts recurring after T-DM1 also overexpressed NRG1 mRNA compared with tumors before treatment (fold change ± SD, untreated = 0.8, SD = 0.5, vs post-T-DM1 = 3.3, SD = 1.1, $P = .02$) (Figure 3C) and exhibited lower levels of HER2 protein (Supplementary Figure 2A, available online). Suggesting a causal association of NRG1 overexpression with drug resistance, exogenous NRG1, but not TGFα or EGF, dampened the cytotoxic effect of T-DM1 in BT474 cells cultured in 3D Matrigel (Supplementary Figure 2, B and C, available online). Further, NRG1 mRNA levels positively correlated with an increased IC_{50} for T-DM1 across the panel of HER2+ cell lines ($R^2 = 0.20$, $P = .04$) (Supplementary Figure 2D, available online). Finally, analysis of KM Plotter web utility (accessed January 26, 2017) showed that overexpression of NRG1 and EGF were associated with poor overall survival in a cohort of 129 patients with HER2+ breast cancer (Supplementary Table 2, available online) (15).

To identify similar correlations in primary tumors, we next analyzed levels of P-HER3, HER2, and NRG1 in a small cohort of 11 matched pre- and post-treatment tumor biopsy pairs from patients with HER2+ breast cancer that had progressed after anti-HER2 therapies including T-DM1 (Supplementary Table 3). HER2 expression and amplification were evaluated by IHC and fluorescence in situ hybridization (FISH), respectively. We observed a reduction of HER2 protein levels in seven of 11 (63.6%) post-T-DM1 tumors (Figure 4A), an increase in P-HER3 in six of 11 (54.5%) post-T-DM1 tumors (Figure 4B), and a statistically significant upregulation of NRG1 transcripts in post-treatment samples (fold change ± SD; pretreatment = 2, SD = 1.9, vs post-treatment = 11.4, SD = 10.3; $P = .04$) (Figure 4C). Of note, two tumors lost detectable HER2 amplification as measured by FISH

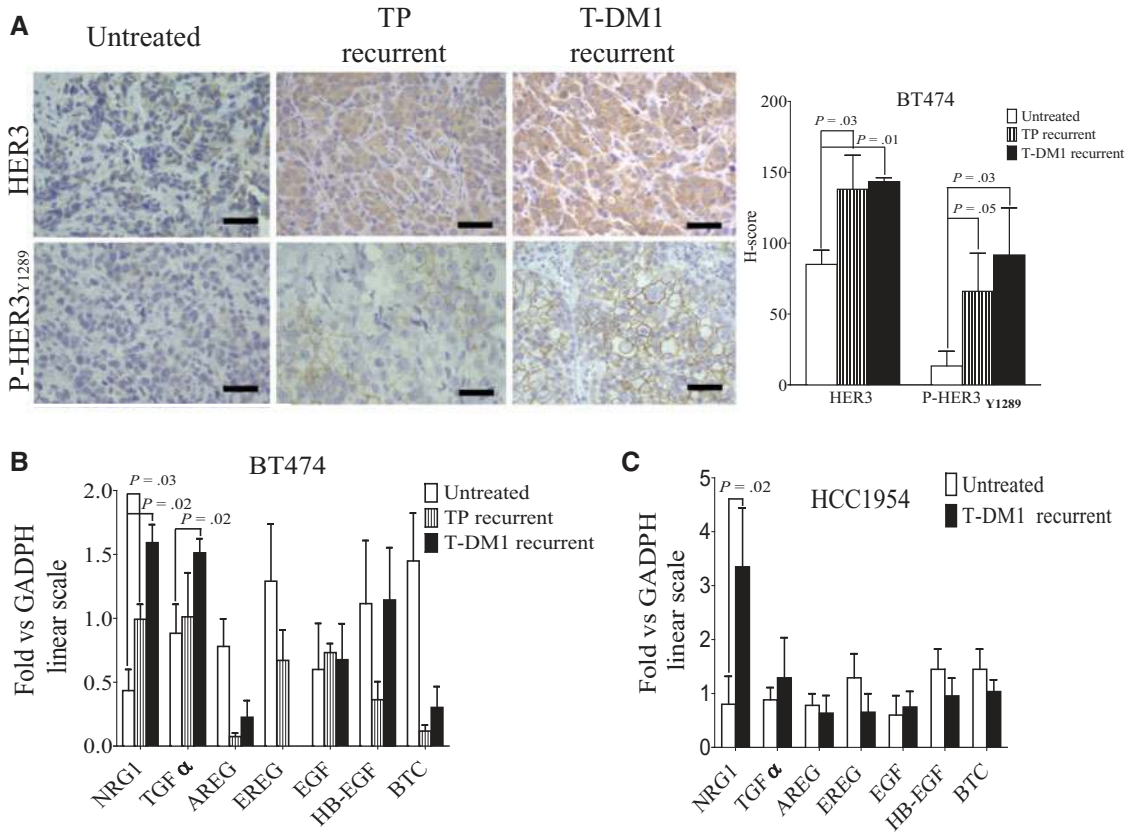

Figure 3. NRG1 and human epidermal growth factor receptor 3 (HER3) expression in Post-TP and T-DM1 recurrent xenografts. **A) Left**: HER3 and P-HER3$_{Y1289}$ immunohistochemistry of formalin-fixed paraffin-embedded sections from BT474 xenografts harvested prior to treatment and after recurrence to TP and T-DM1 (as in **Figure 2A**). **Right**: Histoscores (H-score) were calculated by an expert breast pathologist (MVE) blinded to treatment. **Scale bar** = 200 μm. Post-TP and post-T-DM1 recurrent tumors displayed higher levels of membrane HER3 and P-HER3$_{Y1289}$ compared with untreated BT474 xenografts. Each **bar** represents the mean H-score ± SD (n = 3 for T-DM1 recurrent and n = 2 for TP recurrent). Two-tailed paired and unpaired *t* tests were performed to calculate *P* values for T-DM1 and TP recurrent tumors, respectively. **B and C)** mRNA levels of ERBB ligands were measured by quantitative reverse transcription polymerase chain reaction in BT474 and HCC1954 xenografts harvested prior to treatment and after recurrence following treatment with T-DM1 and TP (as in **Figure 2, A and B**). Each **bar** represents mean ERBB ligand transcript level ± SD relative to GAPDH mRNA (n = 3 for T-DM1 recurrent and n = 2 for TP recurrent). Two-tailed paired and unpaired *t* tests were performed to calculate *P* values for T-DM1 and TP recurrent tumors, respectively. TP = trastuzumab/pertuzumab.

but still exhibited upregulation of P-HER3 and NRG1 mRNA (Figure 4D), suggesting they continued to rely on ERBB receptor activation.

NRG1/HER3 Axis in Breast Cancers With Acquired Resistance to Trastuzumab or T-DM1

We next examined whether other cells resistant to anti-HER2 therapies also upregulated NRG1 and HER3. We interrogated HR6 cells derived from a BT474 xenograft that recurred under continuous trastuzumab treatment (6) and generated HCC1954 and UACC893 cells with acquired resistance to T-DM1 (HCC1954-TDR and UACC893-TDR) in vitro. The IC_{50} values for T-DM1 were greater than five-, greater than six-, and 600-fold in HR6, UACC893-TDR, and HCC1954-TDR cells, respectively, compared with their drug-sensitive counterparts (Figure 5A). All resistant cells had higher HER3, P-HER3, and NRG1 levels compared with their parental controls and maintained robust levels of EGFR and activation of PI3K as evidenced by S473 P-AKT immunoblot analysis of unstimulated cell lysates (Figure 5, B and C). Of note, HCC1954-TDR cells expressed almost undetectable levels of HER2 (Figure 5B). Treatment with the HER3-neutralizing antibody LJM716 (16) resensitized the HR6 and HCC1954-TDR cells to T-DM1 (Figure 5D). Interestingly, the drug-resistant cells remained sensitive to Pan-HER (Supplementary Figure 4, available online). HR6 and HCC1954-TDR cells also contained an expanded cancer stem cell–like (CSC-like) fraction characterized by $CD44^{+}/ALDH^{+}$ cells and enhanced secondary mammosphere formation capacity (Supplementary Figure 5A and B, available online). Treatment with LJM716 or Pan-HER, but not with TP or T-DM1, markedly reduced secondary mammosphere formation by the drug-resistant cells (Supplementary Figure 5C, available online). This effect was more potent with Pan-HER than with LJM716, and in the case of HCC1954-TDR cells, the inhibition by Pan-HER was complete. These data suggest a causal association between an activated NRG1-HER3 autocrine axis and a drug-resistant population with tumor-initiating capacity.

Pan-HER Action Against Tumors Relying on ERBB Ligand–Mediated Autocrine Signaling

We next tested whether by blocking autocrine ERBB receptor signaling Pan-HER would be effective against cells with acquired resistance to anti-HER2 therapies. Trastuzumab-resistant HR6 cells growing in 3D Matrigel remained sensitive to TL and Pan-

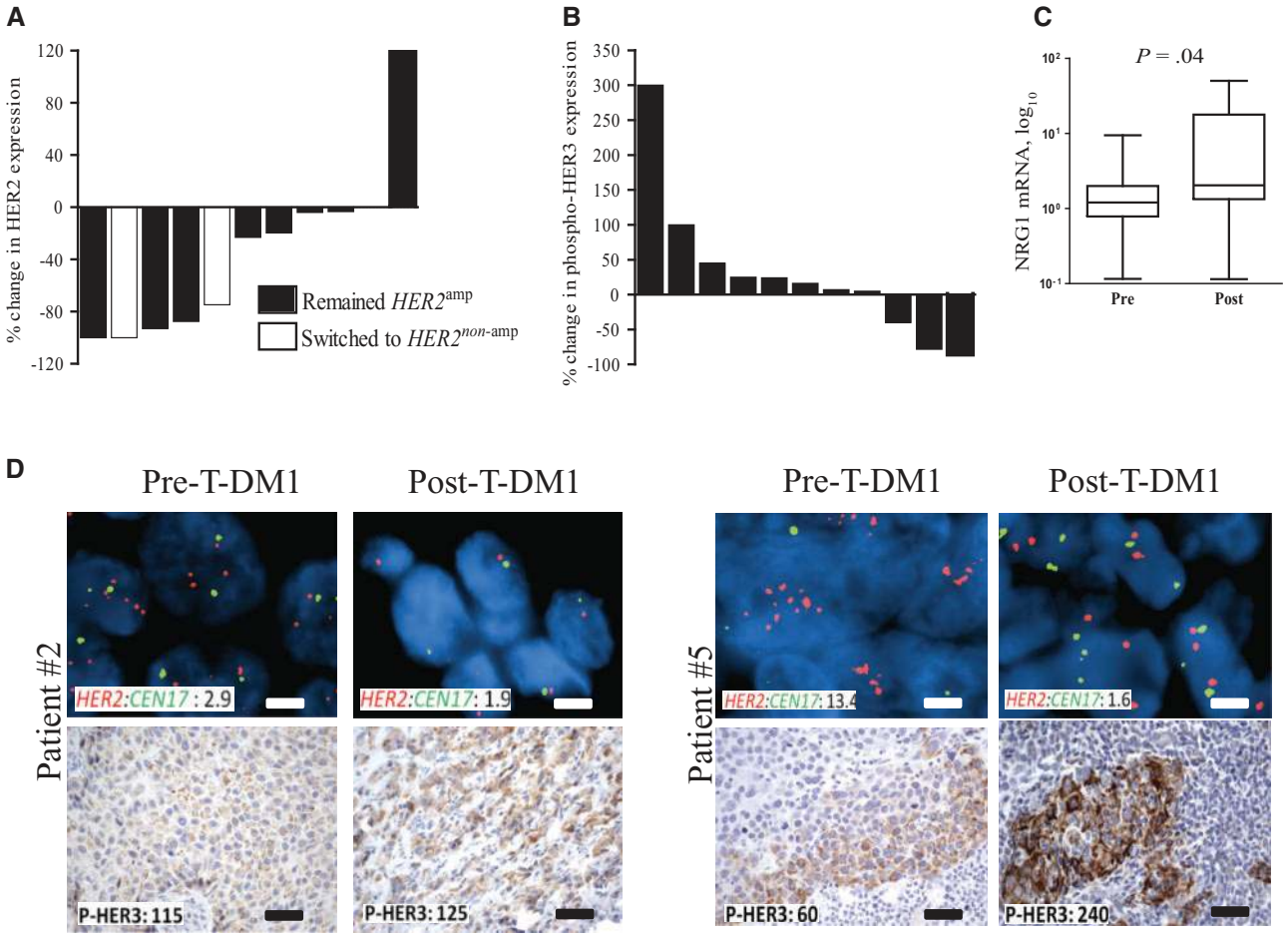

Figure 4. NRG1 mRNA expression upon progression on T-DM1. **A and B)** Percent change of human epidermal growth factor receptor 2 (HER2) and P-HER3$_{Y1289}$ expression measured by histoscores (H-score) in 11 pre- and post-treatment matched tumor biopsies from patients with HER2+ breast cancer. Immunohistochemistry of formalin-fixed paraffin-embedded tumor sections was performed with a C-terminal antibody for HER2. **C)** NRG1 transcript levels were measured by quantitative reverse transcription polymerase chain reaction on RNA extracted from matched paired biopsies described in **(A)**. Each **bar** represents mean NRG1 ligand transcript level ± SD relative to GAPDH, beta-actin, and Rplp0 mRNA (n = 11). **D)** Representative images from two tumors described in **(A)** comparing *HER2*:CEN17 ratio measured by fluorescence in situ hybridization and P-HER3$_{Y1289}$ quantified by H-score before and after progression on T-DM1. **Scale bar** = 50 μm. Two-tailed paired *t* tests were performed to calculate *P* values for T-DM1 and trastuzumab/pertuzumab recurrent tumors, respectively.

HER (Supplementary Figure 6A, available online). However, studies in athymic mice showed that only Pan-HER, but not TL, TP, or T-DM1, arrested HR6 tumor growth ($P < .001$, $P < .001$, and $P = .03$ for Pan-HER vs TL, TP, and T-DM1, respectively) while downregulating EGFR, HER2, HER3, P-HER3, and P-AKT (Figure 6, A and B). HR6 xenografts overexpressed NRG1 ($P = .05$) and TGFα mRNA ($P = .03$) compared with parental BT474 tumors (Figure 6C). Although they maintained *HER2* gene amplification (6), IHC with C-terminal and N-terminal HER2 antibodies suggested they contained lower levels of HER2 protein at the plasma membrane (Figure 6D).

HCC1954-TDR cells were relatively cross-resistant to TL and TP but remained exquisitely sensitive to Pan-HER in vitro (Supplementary Figure 6B, available online). Consistent with these data, HCC1954-TDR tumors established in nude mice responded completely and rapidly to treatment with Pan-HER ($P < .001$) but had an accelerated growth after treated with TL, TP, or T-DM1 (Figure 7A; Supplementary Figure 6C, available online). Mice with large tumors (~1000 mm^3) growing after TL, TP, or T-DM1 were switched to Pan-HER. Of note, only three doses of Pan-HER were enough to rapidly induce complete tumor regressions (Supplementary Figure 6, C and D, available online) and prevent recurrence after up to 200 days of follow-up (Figure 7A).

Immunoblot analysis of Pan-HER-treated HCC1954-TDR tumor lysates corroborated downregulation of EGFR, HER2, HER3, P-HER3, and P-AKT (Figure 7B). NRG1 was the only ERBB ligand upregulated at the mRNA level in HCC1954-TDR tumors (Figure 7C), which no longer exhibited *HER2* gene amplification as measured by FISH (Figure 7D). Loss of HER2 amplification fits the lack of response to T-DM1 whereas their exquisite response to Pan-HER supports the continuous reliance of these drug-resistant tumors on auto-activated HER3/EGFR. Taken together, these data suggest that neutralizing antibody mixtures such as Pan-HER could be a feasible therapeutic strategy in solid tumors with acquired resistance to anti-HER2 targeted therapies.

Discussion

The *HER2* oncogene product is amplified in approximately 20% of invasive breast cancers. Despite advances in the understanding of HER2 biology that have led to approval of four anti-HER2 drugs and the adoption of dual HER2 blockade as the new

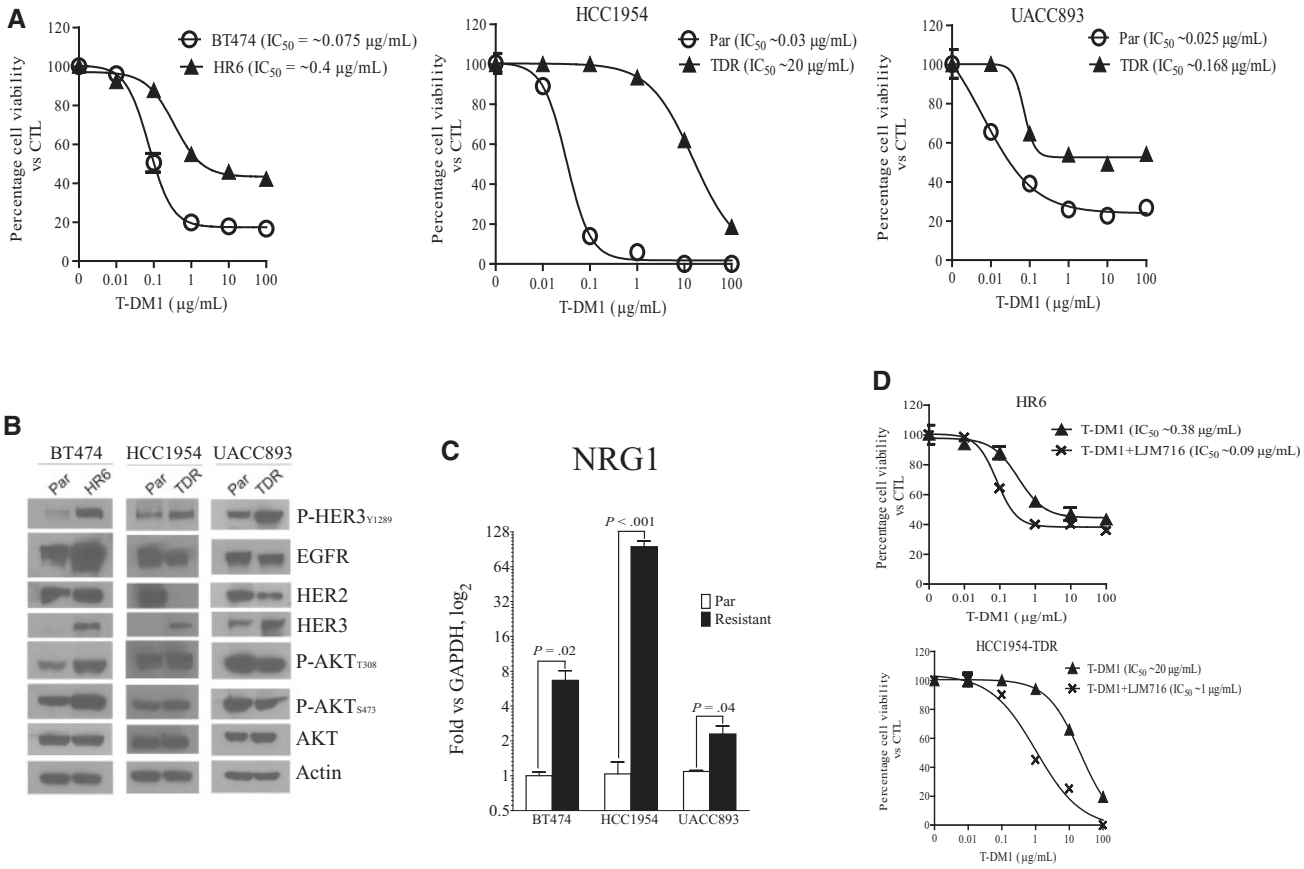

Figure 5. A NRG1–human epidermal growth factor receptor 3 (HER3) autocrine loop in T-DM1-resistant breast cancer cells. **A)** BT474/HR6 (~3x10^3/well), HCC1954 parental/TDR (~1x10^3/well), and UACC893 parental/TDR (~3x10^3/well) cells were seeded in 96-wells in triplicate in their respective growth media and treated with T-DM1 (0.01–100 μg/mL) for three days; cell proliferation was determined using sulforhodamine B (SRB). **B)** Lysates from cells shown in **(A)** were prepared, separated by SDS-PAGE, and then analyzed by immunoblotting with the indicated antibodies. **C)** mRNA levels of NRG1 in BT474/HR6, HCC1954 parental/TDR, and UACC893 parental/TDR cells were measured by quantitative reverse transcription polymerase chain reaction (n = 3). The **y-axis** represents NRG1 transcript levels vs GAPDH mRNA. Two-tailed paired *t* tests were performed to calculate *P* values. **D)** BT474/HR6 (~3x10^3/well) and HCC1954 parental/TDR (~1x10^3/well) cells were seeded in 96-wells in triplicate in their respective growth media and treated with T-DM1 (0.01–100 μg/mL) ± LJM716 10 μg/mL for three days; cell proliferation was determined using sulforhodamine B (SRB). EGFR = epidermal growth factor receptor.

standard of care in firstline treatment of HER2+ breast cancer, there is a cohort of patients with primary and acquired resistance to HER2-directed therapies. Further, although we can control HER2+ metastatic recurrences for a prolonged period of time, anti-HER2 therapies are still not curative in this setting (17–19). Tumor heterogeneity and the plasticity and redundancy of ERBB (HER) receptor family members are among the main reasons for resistance to HER2-targeted therapies (20).

In the present work, HER2+ breast cancer cell lines with acquired resistance to T-DM1 exhibited increased expression and activation of the HER3 coreceptor and its cognate ligand NRG1. This compensatory upregulation of ERBB receptor signaling in HER2+ cells with acquired drug resistance provides targets for alternative treatments. For example, trastuzumab-resistant HR5 and HR6 BT474 tumors with increased expression of EGFR and ERBB ligands respond to the EGFR TKI erlotinib in vivo (6). Along these lines, Rimm et al. reported that in the large North Central Cancer Treatment Group N9831 clinical trial, adjuvant trastuzumab did not improve the outcome of patients with HER2+ breast cancer that also harbored EGFR overexpression measured by automated quantitative analysis (AQUA) system (21). Narayan et al. also reported similar "ERBB reprogramming," where HER2+ breast cancer cells after chronic exposure to trastuzumab in vitro exhibit upregulation of EGFR and HER3 and enhanced sensitivity to EGFR and HER3 inhibitors (11). These adaptive changes in ERBB receptor and ligand expression underscore the plasticity of the ERBB network and its role in acquired drug resistance.

In this work, Pan-HER induced ERBB receptor internalization and degradation in a panel of HER2+ breast cancer cell lines and an equivalent antitumor effect against trastuzumab-naïve HER2+ tumors compared with TL, TP, or T-DM1 in vivo. This effect was independent of the *PIK3CA* mutation status of the tumors, an increasingly recognized mechanism of resistance to anti-HER2 therapies (22–24). In xenografts recurring after TP and T-DM1, as well as in cells with acquired drug resistance (HR6 and HCC1954-TDR), we observed high co-expression of HER3 and its ligand NRG1 with the presence of an expanded cancer stem-like fraction, suggesting a causal association between a NRG1-HER3 axis and the resistant phenotype. Similar results were obtained in a small cohort of patients with HER2-overexpressing breast cancer with available pre- and post-treatment biopsies, where HER3 and NRG1 were upregulated upon progression to multiple anti-HER2 therapies, including T-DM1. A role of HER3 in adaptation and acquired resistance to anti-HER2 therapies in breast cancer is well supported by previous reports (13,25). A NRG1-HER3 autocrine loop driving drug resistance has also been reported in melanoma, ovarian, head

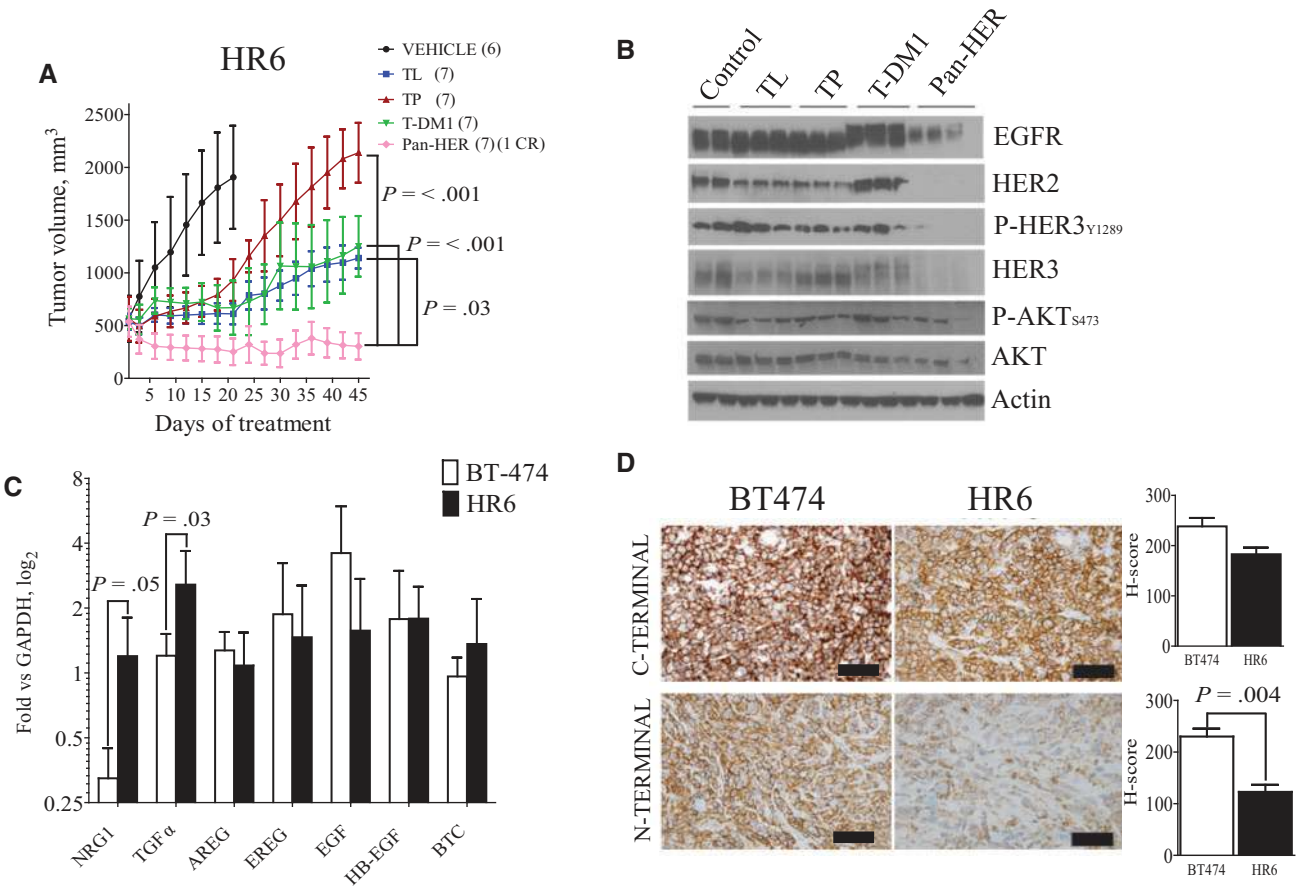

Figure 6. Pan-HER action against trastuzumab-resistant cells and tumors. **A)** HR6 cells were injected subcutaneously into female athymic mice. Once tumors reached a volume of 500 mm^3 or greater, mice were randomly assigned to treatment with vehicle, trastuzumab/lapatinib, trastuzumab/pertuzumab, T-DM1, and Pan-HER as described in **Figure 2**. Numbers of mice per treatment arm are shown **in parentheses**. Tumor diameters were followed serially with calipers and tumor volumes calculated as described in the "Methods" section. Each **data point** represents mean tumor volume in mm^3 ± SD. Paired two-tailed *t* test was used to calculate *P* values. **B)** Xenografts were harvested four hours after the last dose of lapatinib and 24 hours after the last dose of any of the antibodies. Tumor lysates were prepared and analyzed by immunoblotting with the indicated antibodies. **C)** mRNA levels of ERBB ligands measured by quantitative reverse transcription polymerase chain reaction in untreated BT474 and HR6 xenografts. Each **bar** represents the mean transcript level ± SD relative to GAPDH mRNA (n = 6). Two-tailed paired *t* tests were performed to calculate *P* values. **D) Left**: Immunohistochemistry of formalin-fixed paraffin-embedded sections from BT474 and HR6 xenografts using C-terminal and N-terminal HER2 antibodies. **Right**: Histoscores (H-score) were calculated by an expert breast pathologist (MVE) blinded to tumor type. **Scale bar** = 200 μm. HR6 xenografts displayed lower levels of membrane HER2 compared with parental BT474 cells. Each **bar** represents the mean H-score ± SD (n = 7). Paired two-tailed *t* test was used to calculate *P* values. CR = number of complete responses; TL = trastuzumab/lapatinib; TP = trastuzumab/pertuzumab.

and neck, and prostate cancers (26–31). NRG1 has been linked to an increased mammosphere-forming capacity and high MDR1 expression in breast cancer cells, characteristics associated with tumor recurrence and poor prognosis (32,33). Expression of H1047R PIK3CA, an activating mutation in the p110α catalytic domain of PI3K, markedly upregulates NRG1 and attenuates the antitumor effect of trastuzumab and lapatinib against HER2+ breast cancer cells (34), also suggesting that PI3K mutants promote resistance to anti-HER2 drugs by amplifying ligand-induced signaling output of the ERBB receptor network. Further, exogenous NRG1β reduces the cytotoxic activity of T-DM1 in a subset of breast cancer cell lines, and this effect is reversed by the addition of pertuzumab, an antibody that blocks NRG1-induced HER2-HER3 dimerization (10). In line with this observation, treatment with the HER3-neutralizing antibody LJM716 resensitized NRG1-overexpressing drug-resistant cells to T-DM1 in the study we report herein. Finally, treatment with Pan-HER induced ERBB receptor downregulation and regression of T-DM1-resistant HR6 and HCC1954 tumors, and also prevented tumor recurrences after therapy was stopped.

We recognize that this study has some limitations. For example, in addition to NRG1-HER3 axis overexpression, other mechanisms of could be involved in drug resistance, such as expression of p95HER2, a truncated form of HER2 not recognized by any of the HER2 antibodies (35,36). Confirmation that NRG1-HER3 axis overexpression is a major mechanism of escape from T-DM1 and other anti-HER2 therapies will require prospective systematic rebiopsy of a larger number of HER2+ cancers at the time of post-treatment progression and comparison with matched treatment-naïve tumors.

Our results also suggest the possibility that upon resistance to trastuzumab or T-DM1, in some tumors there is marked reduction of HER2 at the plasma membrane and/or a selection of cells without HER2 gene amplification. These scenarios would limit the activity of some treatment sequences such as that of TP after trastuzumab or T-DM1 and of T-DM1 shortly after trastuzumab, for example, because TP and T-DM1 rely on high HER2 expression at the tumor cell membrane in order to exert antibody-dependent, cell-mediated cytotoxicity or adequate internalization for the targeted delivery of chemotherapy,

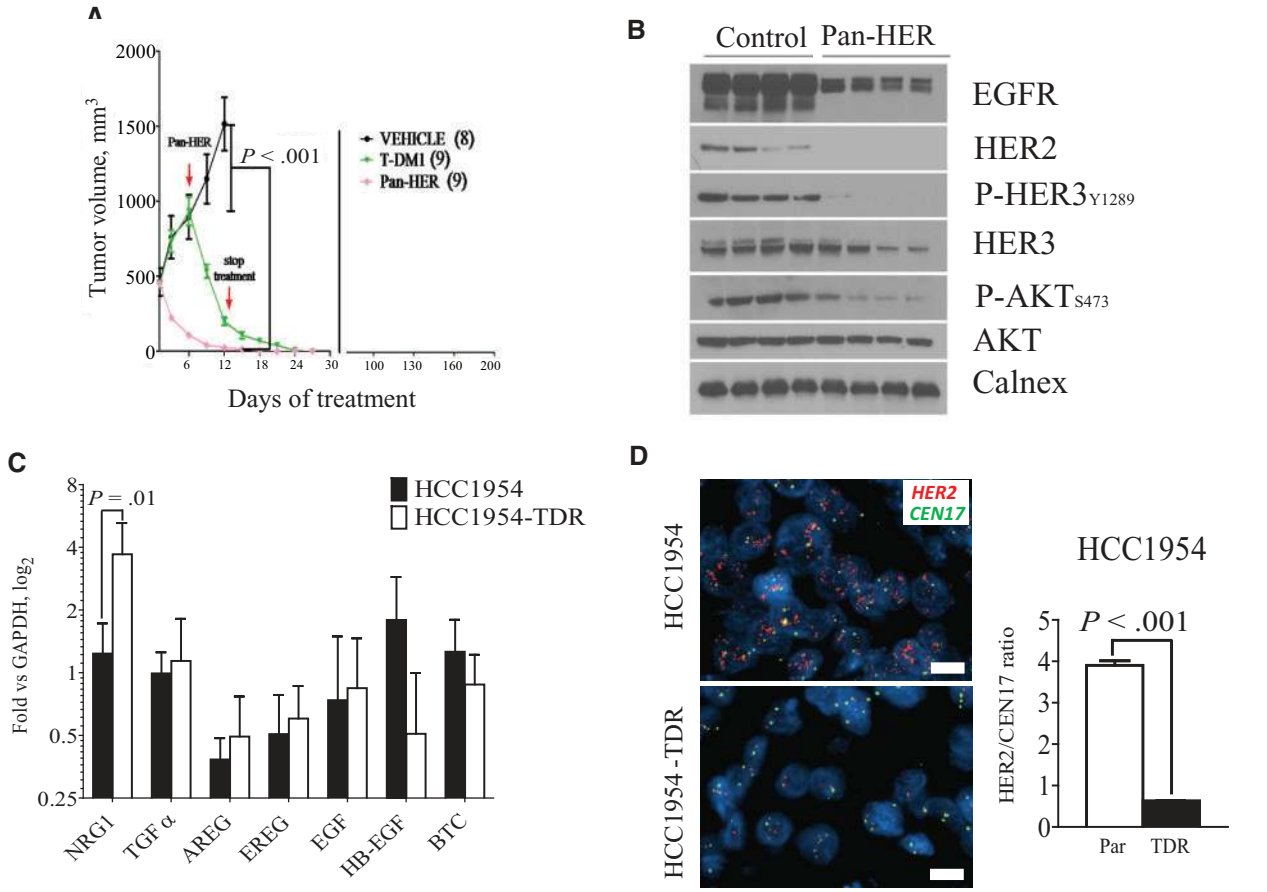

Figure 7. Pan-HER action against T-DM1-resistant xenografts. **A)** HCC1954-TDR cells were injected subcutaneously in the dorsum of female athymic mice. Mice bearing tumors measuring 500 mm^3 or larger were randomly assigned to treatment with 1) vehicle, 2) T-DM1 15 mg/kg intravenously by single tail vein injection, or 3) Pan-HER 50 mg/kg intraperitoneally three times a week. Numbers of mice per treatment arm are shown **in parentheses**. **Arrow** indicates the time at which mice treated with T-DM1 were switched to Pan-HER. Each **data point** represents mean tumor volume in mm^3 ± SD. Paired two-tailed *t* test was used to calculate *P* values. **B)** Xenografts were harvested 24 hours after the last dose of Pan-HER. Tumor lysates were prepared and analyzed by immunoblot with the indicated antibodies. **C)** mRNA levels of ERBB ligands measured by quantitative reverse transcription polymerase chain reaction in untreated HCC1954 and HCC1954-TDR xenografts. Each **bar** represents the mean transcript level ± SD relative to GAPDH mRNA (n = 7). Paired two-tailed *t* test was used to calculate *P* values. **D)** Ratio of HER2:CEN17 signals (~3.9 for TDR vs ~0.6 for parental; **right**) as measured by fluorescence in situ hybridization of formalin-fixed paraffin-embedded sections (**left**) from xenografts presented in **(A)**. **Bars** represent mean ± SD of *HER2*:CEN17 ratio (n = 5). Scale bar = 100 μm. Paired two-tailed *t* test was used to calculate *P* values.

respectively (37–40). If these tumor cells remained dependent on EGFR and/or HER3, multitargeted interventions such as Pan-HER, which simultaneously remove and/or block all ERBB receptors and ligands, would be an effective approach against HER2-overexpressing cancers both sensitive and resistant to anti-HER2 therapies. This approach may also be applicable to other cancers relying on multiple RTK signaling networks.

Funding

This work was supported by National Cancer Institute (NCI) R01 grant CA080195; NCI K08 grant CA143153 (to BNR); American Cancer Society Clinical Research Professorship Award CRP-07-234-06-COUN; National Institutes of Health Breast Cancer Specialized Program of Research Excellence (SPORE) grant P50 CA98131; and Vanderbilt-Ingram Cancer Center Support Grant P30 CA68485.

Notes

The study funders had no role in the design of the study; the collection, analysis, or interpretation of the data; the writing of the manuscript; or the decision to submit the manuscript for publication. Author contributions: CLA and LJS conceived and designed the project. LJS, MVE, PGE, MES, TCD, LF, ALG, MRB, and CDY performed experiments. CLA, LJS, BNR, KEH, LF, and ALG analyzed the data. CLA, LJS, and KEH wrote the manuscript with input from all other authors. All coauthors reviewed and approved both submissions of the manuscript.

JL, MWP, and MK are co-inventors on a patent owned by Symphogen A/S that describes the Pan-HER composition. JL, MWP, MK, and IDH are employees of Symphogen. No potential conflicts of interest were disclosed by the other authors.

References

1. Jacobsen HJ, Poulsen TT, Dahlman A, et al. Pan-HER, an antibody mixture simultaneously targeting EGFR, HER2, and HER3, effectively overcomes tumor heterogeneity and plasticity. *Clin Cancer Res*. 2015;21(18):4110–4122.
2. Francis DM, Huang S, Armstrong EA, et al. Pan-HER inhibitor augments radiation response in human lung and head and neck cancer models. *Clin Cancer Res*. 2016;22(3):633–643.
3. Bertotti A, Papp E, Jones S, et al. The genomic landscape of response to EGFR blockade in colorectal cancer. *Nature*. 2015;526(7572):263–267.
4. Nielsen CH, Jensen MM, Kristensen LK, et al. In vivo imaging of therapy response to a novel pan-HER antibody mixture using FDG and FLT positron emission tomography. *Oncotarget*. 2015;6(35):37486–37499.

5. Motoyama AB, Hynes NE, Lane HA. The efficacy of ErbB receptor-targeted anticancer therapeutics is influenced by the availability of epidermal growth factor-related peptides. *Cancer Res*. 2002;62(11):3151–3158.
6. Ritter CA, Perez-Torres M, Rinehart C, et al. Human breast cancer cells selected for resistance to trastuzumab in vivo overexpress epidermal growth factor receptor and ErbB Ligands and remain dependent on the ErbB receptor network. *Clin Cancer Res*. 2007;13(16):4909–4919.
7. Agus DB, Akita RW, Fox WD, et al. Targeting ligand-activated ErbB2 signaling inhibits breast and prostate tumor growth. *Cancer Cell*. 2002;2(2):127–137.
8. Phillips GDL, Li GM, Dugger DL, et al. Targeting HER2-positive breast cancer with trastuzumab-DM1, an antibody-cytotoxic drug conjugate. *Cancer Res*. 2008;68(22):9280–9290.
9. Scheuer W, Friess T, Burtscher H, Bossenmaier B, Endl J, Hasmann M. Strongly enhanced antitumor activity of trastuzumab and pertuzumab combination treatment on HER2-positive human xenograft tumor models. *Cancer Res*. 2009;69(24):9330–9336.
10. Phillips GD, Fields CT, Li G, et al. Dual targeting of HER2-positive cancer with trastuzumab emtansine and pertuzumab: Critical role for neuregulin blockade in antitumor response to combination therapy. *Clin Cancer Res*. 2014; 20(2):456–468.
11. Narayan M, Wilken JA, Harris LN, Baron AT, Kimbler KD, Maihle NJ. Trastuzumab-induced HER reprogramming in "resistant" breast carcinoma cells. *Cancer Res*. 2009;69(6):2191–2194.
12. Garrett JT, Sutton CR, Kuba MG, Cook RS, Arteaga CL. Dual blockade of HER2 in HER2-overexpressing tumor cells does not completely eliminate HER3 function. *Clin Cancer Res*. 2013;19(3):610–619.
13. Garrett JT, Olivares MG, Rinehart C, et al. Transcriptional and posttranslational up-regulation of HER3 (ErbB3) compensates for inhibition of the HER2 tyrosine kinase. *Proc Natl Acad Sci U S A*. 2011;108(12):5021–5026.
14. Chakrabarty A, Bhola NE, Sutton C, et al. Trastuzumab-resistant cells rely on a HER2-PI3K-FoxO-survivin axis and are sensitive to PI3K inhibitors. *Cancer Res*. 2013;73(3):1190–1200.
15. Gyorffy B, Lanczky A, Eklund AC, et al. An online survival analysis tool to rapidly assess the effect of 22,277 genes on breast cancer prognosis using microarray data of 1,809 patients. *Breast Cancer Res Treat*. 2010;123(3):725–731.
16. Garner AP, Bialucha CU, Sprague ER, et al. An antibody that locks HER3 in the inactive conformation inhibits tumor growth driven by HER2 or neuregulin. *Cancer Res*. 2013;73(19):6024–6035.
17. Baselga J, Cortes J, Kim SB, et al. Pertuzumab plus trastuzumab plus docetaxel for metastatic breast cancer. *N Engl J Med*. 2012;366(2):109–119.
18. Verma S, Miles D, Gianni L, et al. Trastuzumab emtansine for HER2-positive advanced breast cancer. *N Engl J Med*. 2012;367(19):1783–1791.
19. Krop IE, Kim SB, Gonzalez-Martin A, et al. Trastuzumab emtansine versus treatment of physician's choice for pretreated HER2-positive advanced breast cancer (TH3RESA): A randomised, open-label, phase 3 trial. *Lancet Oncol*. 2014;15(7):689–699.
20. Arteaga CL, Engelman JA. ERBB receptors: From oncogene discovery to basic science to mechanism-based cancer therapeutics. *Cancer Cell*. 2014;25(3): 282–303.
21. Rimm D, Ballman KV, Cheng H, et al. EGFR expression measured by quantitative immunofluorescense is associated with decreased benefit from trastuzumab in the adjuvant setting in the NCCTG (Alliance) N9831 trial. *Cancer Res*. 2012;72.
22. Berns K, Horlings HM, Hennessy BT, et al. A functional genetic approach identifies the PI3K pathway as a major determinant of trastuzumab resistance in breast cancer. *Cancer Cell*. 2007;12(4):395–402.
23. Hanker AB, Pfefferle AD, Balko JM, et al. Mutant PIK3CA accelerates HER2-driven transgenic mammary tumors and induces resistance to combinations of anti-HER2 therapies. *Proc Natl Acad Sci U S A*. 2013;110(35):14372–14377.
24. Rexer BN, Arteaga CL. Intrinsic and acquired resistance to HER2-targeted therapies in HER2 gene-amplified breast cancer: Mechanisms and clinical implications. *Crit Rev Oncog*. 2012;17(1):1–16.
25. Sergina NV, Rausch M, Wang DH, et al. Escape from HER-family tyrosine kinase inhibitor therapy by the kinase-inactive HER3. *Nature*. 2007;445(7126): 437–441.
26. Shames DS, Carbon J, Walter K, et al. High heregulin expression is associated with activated HER3 and may define an actionable biomarker in patients with squamous cell carcinomas of the head and neck. *PLoS One*. 2013;8(2): e56765.
27. Buac K, Xu M, Cronin J, Weeraratna AT, Hewitt SM, Pavan WJ. NRG1/ERBB3 signaling in melanocyte development and melanoma: Inhibition of differentiation and promotion of proliferation. *Pigment Cell Melanoma Res*. 2009;22(6): 773–784.
28. Sheng Q, Liu XG, Fleming E, et al. An activated ErbB3/NRG1 autocrine loop supports in vivo proliferation in ovarian cancer cells [Erratum in: *Cancer Cell*. 2010;17(4):412]. *Cancer Cell*. 2010;17(3):298–310.
29. Soler M, Mancini F, Meca-Cortes O, et al. HER3 is required for the maintenance of neuregulin-dependent and -independent attributes of malignant progression in prostate cancer cells. *Int J Cancer*. 2009;125(11):2565–2575.
30. Wilson TR, Lee DY, Berry L, Shames DS, Settleman J. Neuregulin-1-mediated autocrine signaling underlies sensitivity to HER2 kinase inhibitors in a subset of human cancers. *Cancer Cell*. 2011;20(2):158–172.
31. Wilson TR, Fridlyand J, Yan YB, et al. Widespread potential for growth-factor-driven resistance to anticancer kinase inhibitors. *Nature*. 2012;487(7408):505–509.
32. Jeong H, Kim J, Lee Y, Seo JH, Hong SR, Kim A. Neuregulin-1 induces cancer stem cell characteristics in breast cancer cell lines. *Oncol Rep*. 2014;32(3): 1218–1224.
33. Loganzo F, Tan XZ, Sung M, et al. Tumor cells chronically treated with a trastuzumab-maytansinoid antibody-drug conjugate develop varied resistance mechanisms but respond to alternate treatments. *Mol Cell Therapeut*. 2015;14(4):952–963.
34. Chakrabarty A, Rexer BN, Wang SE, Cook RS, Engelman JA, Arteaga CL. H1047R phosphatidylinositol 3-kinase mutant enhances HER2-mediated transformation by heregulin production and activation of HER3. *Oncogene*. 2010;29(37):5193–5203.
35. Anido J, Scaltriti M, Bech Serra JJ, et al. Biosynthesis of tumorigenic HER2 C-terminal fragments by alternative initiation of translation. *EMBO J*. 2006; 25(13):3234–3244.
36. Scaltriti M, Rojo F, Ocana A, et al. Expression of p95HER2, a truncated form of the HER2 receptor, and response to anti-HER2 therapies in breast cancer. *J Natl Cancer Inst*. 2007;99(8):628–638.
37. Baselga J, Cortes J, Im SA, et al. Biomarker analyses in CLEOPATRA: A phase III, placebo-controlled study of pertuzumab in human epidermal growth factor receptor 2-positive, first-line metastatic breast cancer. *J Clin Oncol*. 2014; 32(33):3753–3761.
38. Schneeweiss A, Chia S, Hegg R, et al. Evaluating the predictive value of biomarkers for efficacy outcomes in response to pertuzumab- and trastuzumab-based therapy: An exploratory analysis of the TRYPHAENA study. *Breast Cancer Res*. 2014;16(4):R73–R73.
39. Baselga J, Phillips GDL, Verma S, et al. Relationship between Tumor Biomarkers and Efficacy in EMILIA, a Phase III Study of Trastuzumab Emtansine in HER2-Positive Metastatic Breast Cancer. *Clin Cancer Res*. 2016; 22(15):3755–3763.
40. Perez EA, Hurvitz SA, Amler LC, et al. Relationship between HER2 expression and efficacy with first-line trastuzumab emtansine compared with trastuzumab plus docetaxel in TDM4450g: A randomized phase II study of patients with previously untreated HER2-positive metastatic breast cancer. *Breast Cancer Res*. 2014;16(3).